# Power producing buoy for strategic applications: Prototype and Testing – Q2 Report

Grant No. HR0011-09-2-0002

Lead Organization: Monterey Bay Aquarium Research Institute
7700 Sandholdt Road
Moss Landing, CA 95039

Technical points of contact: Andrew Hamilton, Ph.D.
Jim Bellingham, Ph.D.
Tel: 831-775-1861/831-775-1731
Fax: 831-775-1646
Email: hamilton@mbari.org; jgb@mbari.org

Administrative points of contact:
Susan Lantis
Grants Office – MBARI
Tel: 831-775-1803/831-775-1788
Fax: 831-775-1620
Email: grants@mbari.org

Project Period: 3/26/2009-3/25/2011

Report Period: 6/26/2009-9/25/2009

# Summary

In the second quarter of this project, an at-sea test was performed to validate the accuracy of the numerical model developed previously to model floating systems typical of wave-energy extraction devices. The tests were performed on August 10th and 11th, 2009. The data collected during these tests has been analyzed and compared to the model predictions for the deployed system in the wave conditions present on the days of the tests. A summary of these results are presented in this report and a more detailed account of the testing procedure and results analysis is attached as a separate report. In addition to performing an experiment to validate the numerical model in the simple case of a submerged plate, the model capabilities have been extended to include the case of a submerged foil tethered to a surface expression. This configuration is expected to generate thrust when the waves cause the system to heave and the model demonstrates this thrust behavior. Some refinement of the submerged foil case is ongoing and initial results to size a prototype system are being developed. Finally, preliminary work has begun to investigate candidate power take-off systems for the case of a floating surface expression tethered to a submerged element. The numerical model can include the characteristics of the power take-off system and so models of candidate power take-off systems are being developed for inclusion in the numerical motion models. This combined model will provide the capability to predict the power generation capabilities of candidate concepts in various sea-states. Coupling these predictions with the previously generated statistics of wind, wave, and currents at various global sites will provide a long-term prediction of power generation capabilities.

# Activities

1. Performed at-sea test of the behavior of a surface buoy tethered to a submerged plate with a spring/damper system.
2. Performed numerical modeling of deployed system in wave-conditions present at the time of the tests.
3. Extended numerical model to include the characteristics of a submerged foil and generated initial results.
4. Beginning to study power take-off techniques that may be applicable to submerged foil concept.
5. Hamilton attended the 8th European Wave and Tidal Energy Conference (Sept 7-9, Uppsala, Sweden).
6. Hamilton and Bellingham attended Khine Latt's vent power meeting (August, 18th, San Diego, CA).

# Technical Status and Results

## *Model Validation Experiments*

The test device consists of a 92" diameter surface float connected to a submerged element by a hydraulic ram that behaves like a spring/damper system. The main elements are shown in figure 1. The system is instrumented with force and elongation sensors on the tether, the time signals of these measurements provide the main comparison between the experimental measurements and the numerically computed results for a system of the same characteristics (size, weight, spring/damper behavior, etc).

Because the response of the system depends on the input wave field, the tests were performed near a wave height sensing buoy in Monterey Bay. The sea state differed between the two test days, with an approximately 1.5m significant wave height on August 10th and somewhat calmer conditions on August 11th. Figure 2 shows the measured wave height on August 10th during the portion of the day in which the flat plate was being tested below the buoy. In order to incorporate the measured wave-field into the numerical model, the measured time-series data is converted to a power spectrum in the frequency domain; this spectrum is then used to compute the wave elevation used for the numerical computations. Although it would be possible to use the measured wave-height time history directly in the model, the conversion to a wave spectrum and back again allows more information about the incoming wave-field to be used in the model. For instance, the measured wave-height history does not provide the velocity field below the waves, but the velocity field can be determined for a wave-height time series numerically constructed from a spectrum. Use of this technique means that the measured elongations and loads won't match the modeled results on a wave-by-wave basis, but statistically the results should match. For this reason the comparison between measured and modeled results are best done as a comparison of power spectrum for the measured quantities. Time history plots can be useful to provide a general feel for the agreements, but the power spectrum comparisons provide a more quantitative comparison. Figure 3 shows a comparison between the measured (blue) tensions and elongation with those predicted by the model in the same sea-state (red). Decent agreement was found and the discrepancy appears to be mainly due to difficulties in estimating and modeling the damping behavior of the hydraulic spring/damper system.

In general there is sufficient agreement between the modeled and measured results that the model has been validated for use in evaluating concepts for wave-energy extraction and station keeping behaviors for systems at the target size. This is an important result because the modeling techniques make several assumptions that are widely held to be valid for large structures, but were questionably valid for structures at the size scales of interest in this project. More detailed results and explanation are contained in the attached report (*Time Domain Model Validation Results*).

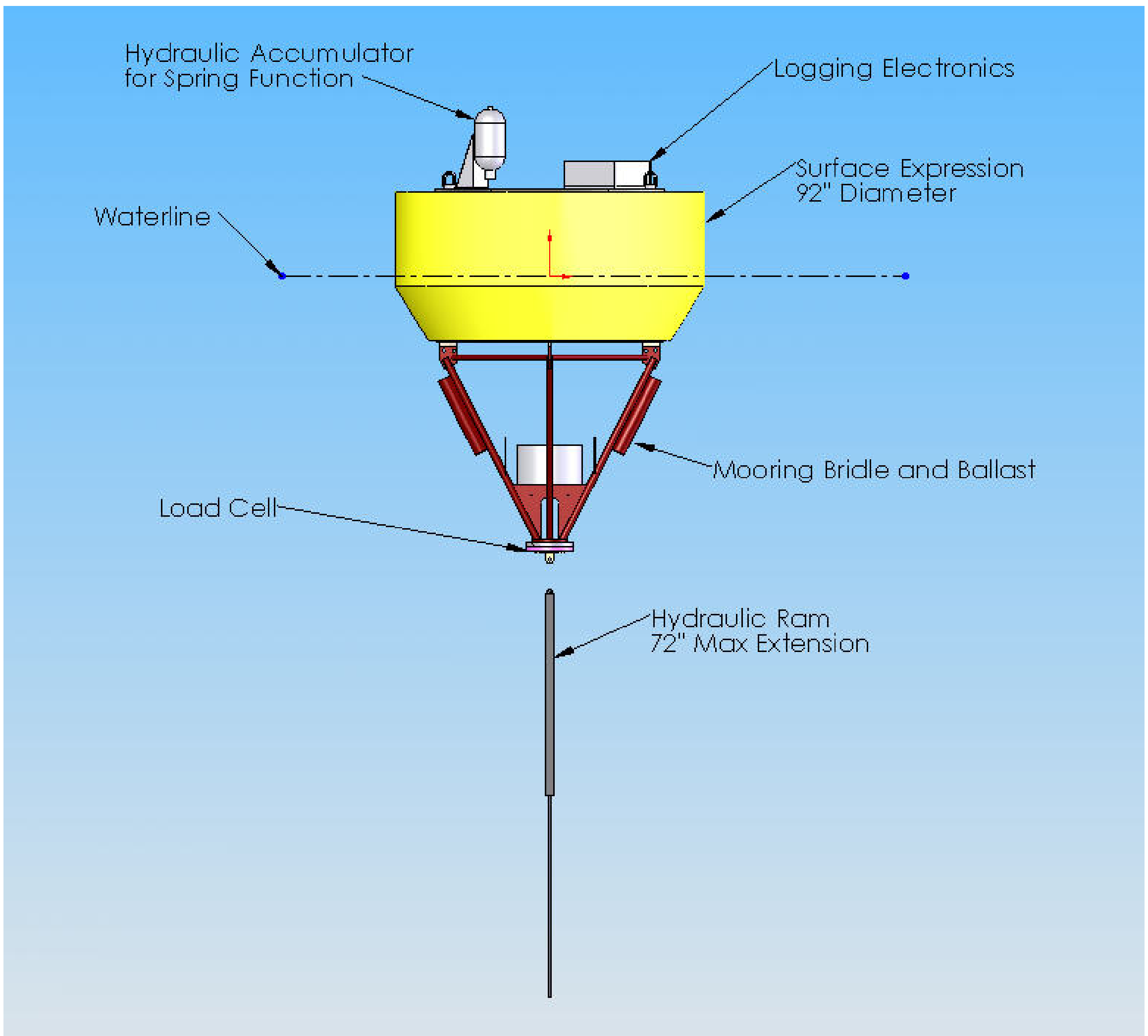


Figure 1: Surface expression and hydraulic cylinder acting as spring/damper system. Two submerged elements (not shown) were tested separately at a depth of 20 meters, a flat plate of 4' diameter and a sphere of 28" diameter.

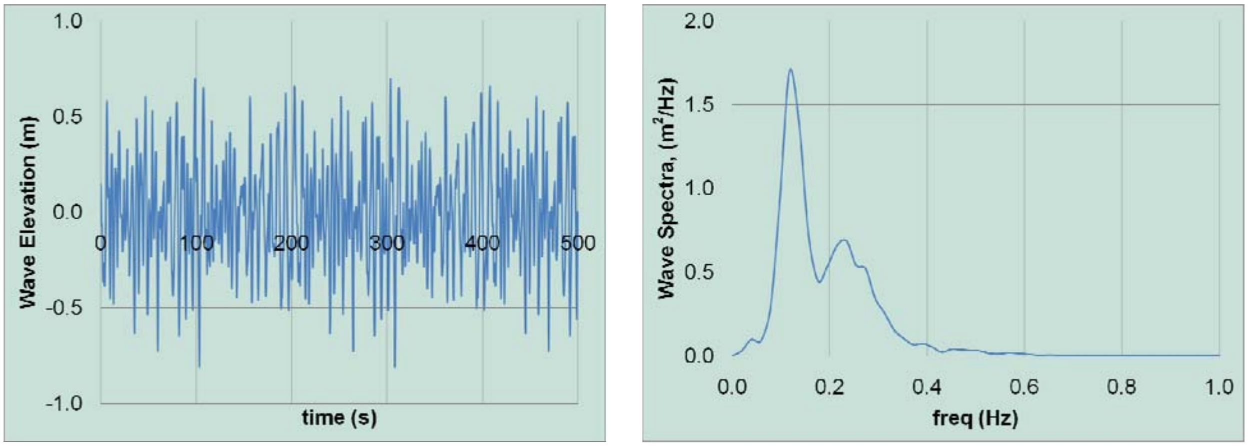


Figure 2: Measured wave height on August 10th, 2009.

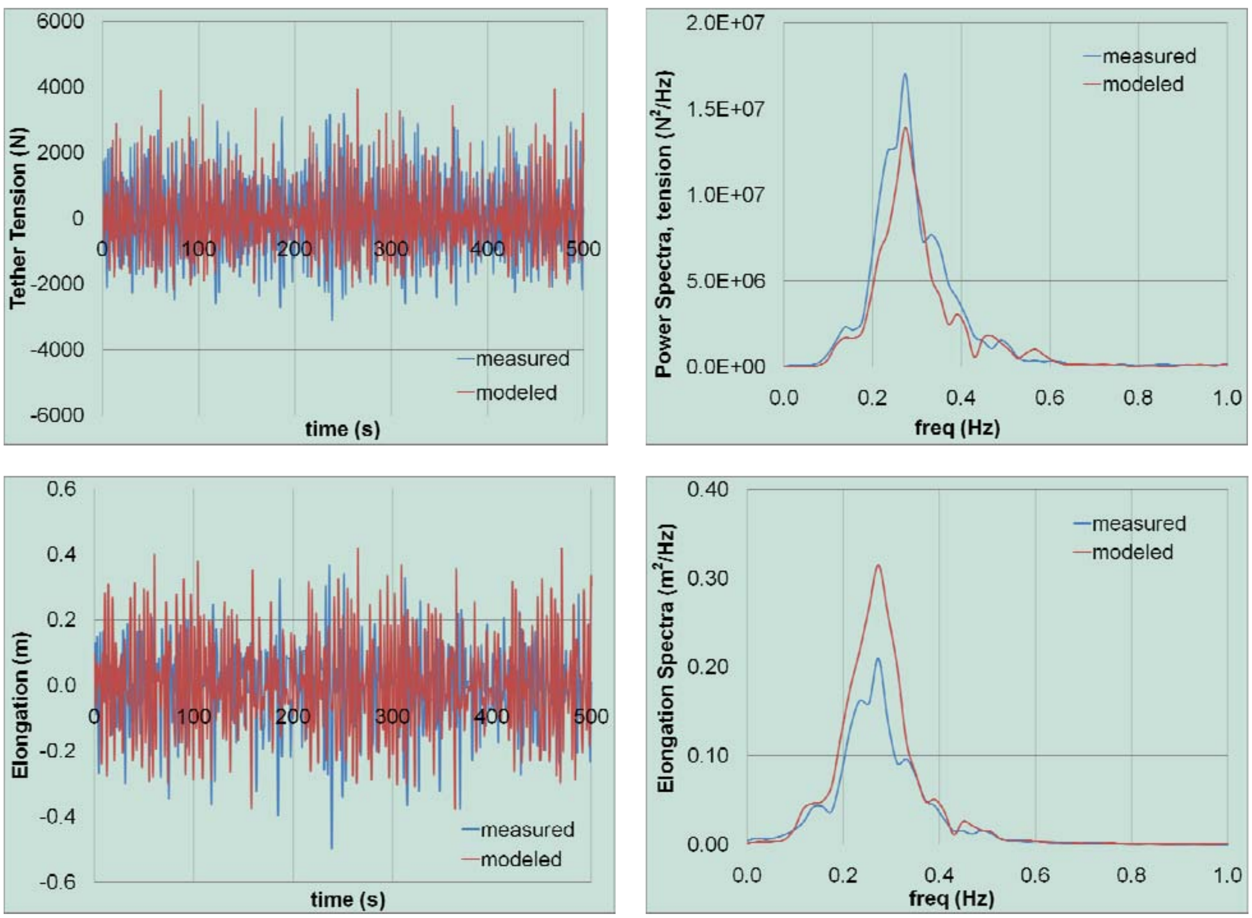


Figure 3: Comparison of measured and modeled tension and elongation behavior for test system. This configuration is for the flat-plate suspended 20m below the buoy on August 10th, 2009. The mean values of the tension and elongation have been subtracted to allow the power spectrum to be computed without a large zero-frequency component.

### *Submerged Foil Results*

A leading concept for realizing a station keeping buoy that produces electrical power involves a surface expression tethered to a submerged foil as shown in Figure 4. In this concept the heaving of the surface expression due to waves drives a submerged foil which produces in a net propulsive force. On a small scale this concept has been demonstrated to effectively propel a very small surface expression at a knot or two (Liquid Robotics). In principle it should also be possible to generate electricity by a power take-off mechanism that relies upon the relative motion of the surface expression and the submerged foil. The immediate goal of this project is to perform sufficient analysis to determine the capabilities of this concept with regard to station keeping and electrical power generation.

Performance predictions for this type of arrangement are possible using the computer code previously developed and validated. In this case the flow over the submerged foil is a lifting flow and necessarily relies on the effects of viscosity to generate propulsion. This complicates the analysis considerably and requires computational fluid dynamics techniques to accurately predict. Airflow Sciences Inc. has been enlisted to perform the required calculations in a manner that can be coupled with the code developed within this project to predict the surface buoy motions and the resulting forces on the tether. It is not immediately clear how sophisticated this modeling needs to be and currently work is underway to evaluate the applicability of several simplifying assumptions that could reduce the effort required. In particular, it's not clear if the analysis can be performed in a "quasi-static" manner, or if a full transient solution will be required.

As a first step in this analysis, before including the sophisticated CFD results, motion results have been computed by assuming that the flow over the foil can be assumed to behave quasi-statically and that the resulting forces are well represented by traditional lift and drag coefficients. In this application the angle of attack of the flow towards the foil is not constrained to a small range near zero as it is in aircraft applications and it is necessary to use tests results that cover all angles of attack, a reasonably complete tabulation of such results are presented in a Sandia National Laboratories report. Figure 5 shows the lift and drag coefficients for a NACA0015 foil shape at a Reynolds number of $1X10^6$. Using these lift and drag estimates in the motion prediction code demonstrates the potential effectiveness of this propulsion technique. An animation of representative results can be found at www.mbari.org/staff/hamilton/Videos/FoilExample.mpg. In this animation the foil in the lower left pane is connected to the surface buoy in the upper left pane. As time progresses the heaving of the foil causes the foil to move to the right and drag the buoy along behind it. The figure in the lower right of the animation shows the apparent inflow to the foil (blue arrow) and the resulting forces on the foil (red when the result is a drag force and green when the result is a propulsive force).

In the example shown in the animation the buoy and foil sizes are comparable to those used in the validation tests performed previously and the spring/damper system in the model corresponds to that used in the validation tests. Additionally, some pitch control has been added to keep the foil oriented advantageously, this is done as an expedient because the foils pitch moments are not available across the range of angles of attack. When the CFD results are used in place of the lift/drag coefficients used here, the dynamics of a simple pitch control mechanism will be included in the model. In the meantime, these results from a simplified model are useful for an initial exploration of the design space. Computations are currently being performed to evaluate the effects of buoy size, foil size, and power take-off characteristics on the system in a range of sea conditions.

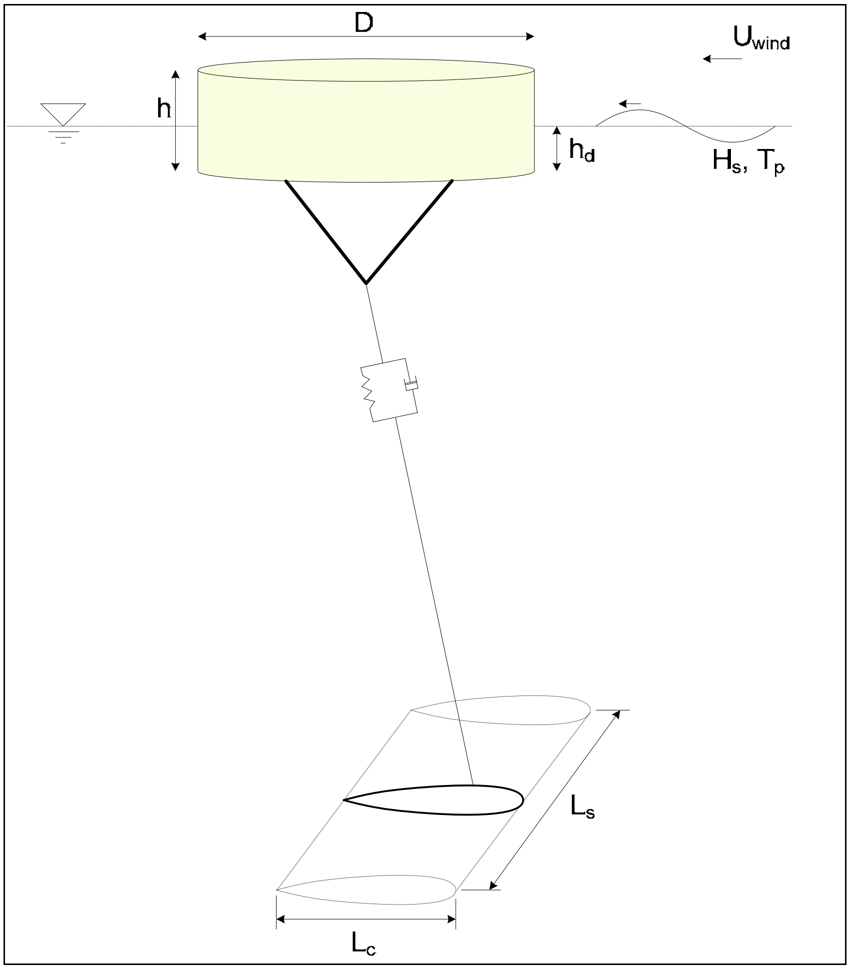


Figure 4: Schematic representation of submerged foil propulsion and power take-off concept.

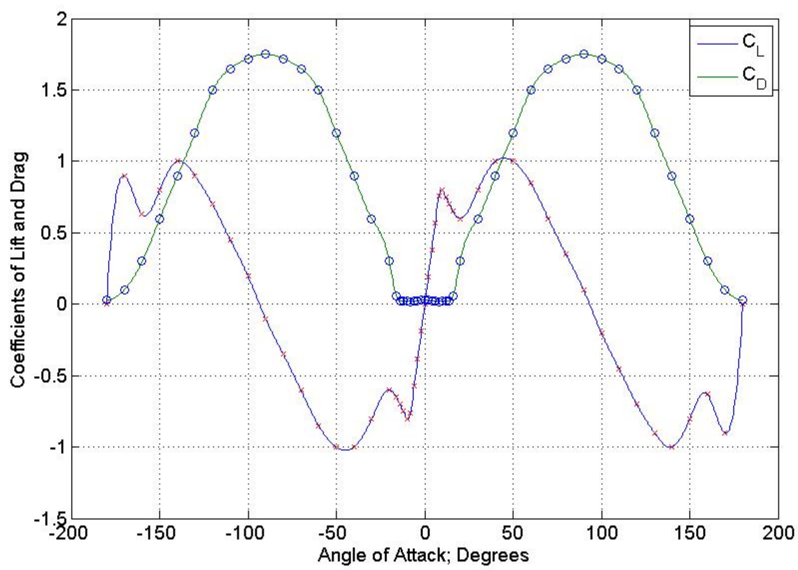


Figure 5: Lift and drag coefficients across all possible angles of attack for a NACA0015 foil section at Re = $1X10^6$ (Sheldahl, Klimas, 1981).

## *Power Take-off Mechanisms*

For the submerged foil concept, the most obvious possibility for electrical power generation in this scheme is a linear generator that takes advantage of the relative motion of the buoy and submerged element as the waves cause the two to oscillate. Linear generators are notoriously inefficient due to the slow speeds they typically operate. Nevertheless, it is possible to generate power in this manner as has been demonstrated by various utility power wave-energy pilot projects.

Although the connection between the submerged element and the buoy is shown as a linear spring and damper in Figure 4, the actual behavior of this element is more complicated and depends on its design and power take-off characteristics. For any particular power take-off device, the characteristics of the device can be included in the numerical model and the resulting performance and electrical power generation potential can be predicted within the limits of the characterization of the power take-off device.

Within the context of this project two novel linear generator technologies have been investigated, one using a proprietary lubricant that has a high magnetic permeability (Ferro-fluid), and another that uses a polymer material that acts as a capacitor of variable thickness (SRI, artifical muscle). Both of these options are at the research stage and aren't directly applicable although the SRI artificial muscle material deserves more investigation. In particular, SRI has indicated that they would be able to predict their materials behavior if provided a motion and force profile. The numerical model developed in this project appears to be the tool they're missing to design and implement a wave-energy device that uses the artificial muscle so further collaboration may be possible.

A more traditional and well understood linear generator technology for this application is a hydraulic system that uses the pumping of a working fluid to rotate the shaft of a traditional electrical generator. This type of system is currently being implemented for utility scale wave-energy pilot projects. For the station-keeping buoy application, the types of hydraulic motors being used in the large scale applications are inappropriate due to their losses at low flow speeds. Figure 6 shows the typical efficiencies of different turbine designs as a function of flow speed (measured as a nondimensional "specific speed"). For the flow rates expected from a device of the size being considered in this project, the specific speed will be relatively low, down in the Pelton wheel range of specific speed as shown in Figure 6. This is a relatively unexplored area of power take-off mechanism for wave-energy devices and work has begun in this project to investigate this type of turbine device for application to the power-buoy device. In particular, a numerical model of a hydraulic power take-off device based on a Pelton wheel turbine is being developed to include in the numerical modeling of the entire system. To ensure validity of this model, laboratory testing is being performed with the hydraulic system from the validation test platform. If the numerical results and testing indicate that electricity can be generated in this manner, the validation test system may be re-deployed in the third quarter of the project to demonstrate electrical generation and to gain experience with the issues surrounding electrical power generation from the platform.

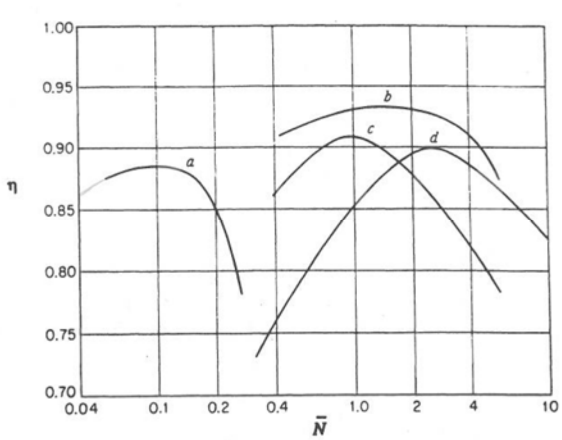


Figure 6: Efficiencies of various turbine types based on specific speed parameter. (a) Pelton wheel, (b) Francis propeller turbine. (c) Centrifugal pump (d) Axial compressors. (from *Fluid Dynamics and Heat Transfer of Turbomachinery*, Lakshminarayana, 1996)

## Budget and Spending

As of 9/25/2009, $128,863 has been spent out a budgeted $654,244. The spending rate for this project is expected to increase significantly at this point as labor resources from the companion project are being concentrated on this project and as additional MBARI staff is added at the beginning of calendar year 2010. Additionally, the outside services budget has been largely unspent so far but that will soon change as the CFD work by Airflow Sciences begins in earnest. Attached to this report is the MBARI budget status report as of 9/25/2009 for this project.

## Attachments

1. Technical Report: *Time Domain Model Validation Results*
2. MBARI Grant Status Report

# Projection Groups: Reports

Project List | Select Projection | Report Groups | Commitments | Logout

Export to Excel

## 707976

| Projection Name | Project |
|---|---|
| 707976.00 | 707976.00 - Power Buoy:Prototype Test |
| 707976.01 | 707976.01 - ***Force&MotionTransdu |
| 707976.02 | 707976.02 - Equip:Wav.Ht.Meas.Buoy |

## Time (in Hours)

| Individual | Line Label | Rate | Actual | 9/09 | Total |
|---|---|---|---|---|---|
| ENG-Institute Mech Tech | | $37.13 | 11.00 | - | **11.00** |
| ENG-Mechanical (TERM) | | $36.06 | 232.00 | - | **232.00** |
| ENG-Systems Engineer | | $66.07 | 142.00 | - | **142.00** |
| SCI-Engineering Assist (TERM) | | $14.05 | 327.00 | - | **327.00** |
| **Total Time** | | | **712.00** | **0.00** | **712.00** |

## Cost

| Line Item | Budget | Actual | Committed | 9/09 | Total | Remaining |
|---|---|---|---|---|---|---|
| 1500-560 \| General Equipment Addtns | $47,608 | - | - | - | **$0** | **$47,608** |
| 1500-568 \| Ocean Deployed Equip Addt | - | $53,856 | - | - | **$53,856** | **($53,856)** |
| 5030-000 \| Conference Fees/Registrat | - | $877 | - | - | **$877** | **($877)** |
| 5120-000 \| OS - External Ship Time | - | $2,860 | - | - | **$2,860** | **($2,860)** |
| 5130-000 \| OS - General | $247,000 | $2,771 | - | - | **$2,771** | **$244,229** |
| 5200-000 \| Postage/Shipping | $336 | $513 | - | - | **$513** | **($177)** |
| 5300-000 \| Supplies - Cmptr/Hdwr | - | $3,701 | - | - | **$3,701** | **($3,701)** |
| 5310-000 \| Supplies - Cmptr/Sftwr | - | $757 | - | - | **$757** | **($757)** |
| 5330-000 \| Non-Capitalized Equipment | - | $395 | - | - | **$395** | **($395)** |
| 5360-000 \| Supplies - General | $31,755 | $2,264 | - | - | **$2,264** | **$29,491** |
| 5500-000 \| Travel - Domestic | $18,900 | $733 | - | - | **$733** | **$18,167** |
| 5530-000 \| Travel - Foreign | - | $2,447 | ($1,448) | - | **$999** | **($999)** |
| Labor | $67,814 | $22,585 | - | - | **$22,585** | **$45,229** |
| Fringe | $35,941 | $10,028 | - | - | **$10,028** | **$25,913** |
| Overhead | $204,890 | $25,078 | ($739) | - | **$24,339** | **$180,551** |
| **Total** | **$654,244** | **$128,863** | **($2,187)** | **$0** | **$126,676** | **$527,568** |

# Time Domain Model Validation Results

## Introduction

In order to analyze the behavior of various wave-energy extraction devices, a general purpose numerical model has been developed that can be configured to model different design concepts. Because this model makes a number of simplifying assumptions, it's important to validate the results of a typical system against experimental results. This report outlines and compares the numerical and experimental results for a simple case of a floating buoy that supports a submerged heavy body 20 meters below the buoy. The two bodies are connected by a hydraulic ram system that behaves like a damped spring element. To validate the model, this system was deployed in Monterey Bay on August 10th and 11th, 2009. The sea state during the tests and the resulting motions of the system were measured and recorded. Subsequent to this experiment the numerical model was run using the sea state from the test days as an input and the results were compared. In addition to the at-sea testing, a step response test of the system was performed in the MBARI test-tank, which consisted of dropping the buoy from a small elevation and measuring the resulting tension and elongation step response.

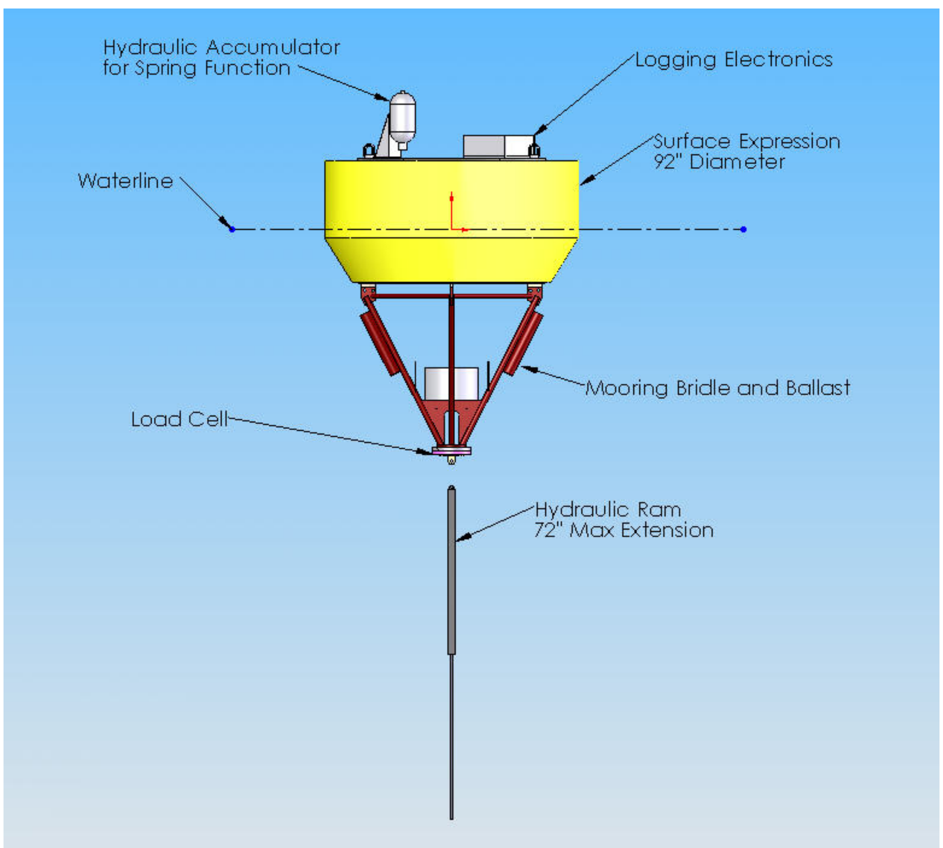


Figure 1: Surface expression and hydraulic cylinder acting as spring/damper system. Flat plate or sphere is connected and submerged at a depth of 20 meters.

# Experimental Set-Up

The experimental set-up consists of a cylindrical surface float and a submerged element that is connected by a hydraulic ram system that behaves as a spring element. Figure 1 shows the surface-buoy configuration. Two different submerged elements were used, a 48” diameter flat plate and a 28” diameter sphere. These two elements were used to provide some variation in the device configuration; the numerical model was run in both configurations as well. The details of the two configurations that were tested are outlined below:

**Configuration I**

Floating Body: MOOS Buoy

- Total Mass: 2600 lbs (1179.34 kg)
  (includes Hydraulic ram, Instruments, Accumulators, Heave Sensor and Bridle assembly)
- Waterline: 4 inches (0.1016 m) above Chine (Location of Origin)
- Center of Gravity: [0, 0, -0.63m]
- Center of Buoyancy: [0, 0, -0.26m]
- Displacement: 1.64 $m^3$
- Moment of Inertia about Origin
  $I_{xx}$ = 1998.19 kg $m^2$
  $I_{yy}$ = 1947.66 kg $m^2$
  $I_{zz}$ = 466.13 kg $m^2$
- Tether Point of Attachment: 2.0 m below chine (2.09 m below waterline)
- Tether Length = 3.0m (test-tank tests), 20.0m (at-sea tests)

Submerged Body: Flat Circular Plate

- Total Mass: 1297 lbs (588.31 kg)
- Radius: 2 ft (0.6096 m)
- Thickness: 2.5 inches (0.0635m)
- Displacement: 0.074133 $m^3$
- Center of Gravity: [0, 0, 0]
- Center of Buoyancy: [0, 0, 0]
- Moment of Inertia about Origin
  $I_{xx}$ = 55.22 kg.$m^2$
  $I_{yy}$ = 55.26 kg.$m^2$
  $I_{zz}$ = 110.08 kg.$m^2$
- Tether Point of Attachment = (54.25 inches) 1.37795 m above CG of plate

**Configuration II**

Floating Body: MOOS Buoy

- Total Mass: 2600 lbs (1179.34 kg)
  (includes Hydraulic ram, Instruments, Accumulators, Heave Sensor and Bridle assembly)
- Waterline: 2.25 inches (5.715 cm) above Chine
- Center of Gravity: [0, 0, -0.63m]
- Center of Buoyancy: [0, 0, -0.29 m]
- Displacement: 1.475 $m^3$

- Moment of Inertia about Origin
  $I_{xx}$ = 1998.19 kg.m $^2$
  $I_{yy}$ = 1947.66 kg.m $^2$
  $I_{zz}$ = 466.13 kg.m $^2$
- Tether Point of Attachment: 2.0 m below chine (2.09 m below waterline)
- Length of tether: 20m (at-sea tests)

<u>Submerged Body No. 2: Solid Sphere</u>
- Total Mass: 1175 lbs (532.97 kg)
- Radius: 14 inches (0.3556 m)
- Displacement: 0.0188354 m $^3$
- Center of Gravity: [0, 0, 0]
- Center of Buoyancy: [0, 0, 0]
- Moment of Inertia about Origin
  $I_{xx}$ = 26.958 kg.m $^2$
  $I_{yy}$ = 26.958 kg.m $^2$
  $I_{zz}$ = 26.958 kg.m $^2$
- Tether Point of Attachment = (14 inches) 0.3556 m above CG of sphere.

**Hydraulic System Description**
The spring/damper system is constructed from industrial hydraulic components, a 72" long linear ram provides compliance and is plumbed to a system of accumulators and valves that provides a spring effect (force proportional to displacement) and a damping effect (force proportional to velocity). Because it is difficult to construct a perfectly linear spring and damper system from these hydraulic components, the actual characteristics of the spring/damper system was measured for inclusion in the numerical model. Figure 2 depicts a schematic representation of the hydraulic system designed and used in the validation experiment. Three accumulators of capacities 1 quart, half gallon and one gallon with precharges 50, 200, 500 psi respectively, provide the required spring force. A pressure sensor (P1) was connected to measure the pressure in the system which is proportional to the tension in the tether.

The spring force in the system is a result of the gas being compressed in the accumulators as the piston rod extends, this is not a linear phenomenon but the three accumulators in parallel approximate a linear spring as shown in the measured force versus elongation results (Figure 3). This measured spring relationship is what is used in the numerical model.

The measured damping force present in the experimental set-up is shown in figure 4, this highly nonlinear damping relationship is approximated for purposes of inclusion in the model in terms of elongation rate '$v$' as

$$Fd = \frac{\Delta F}{2}\left(1 - \exp(-\alpha v)\right) sign(v) \qquad (3)$$

where
$\Delta F$ = mean damping force in N/(m/s)
$\alpha$ = velocity slope coefficient (1/(m/s))

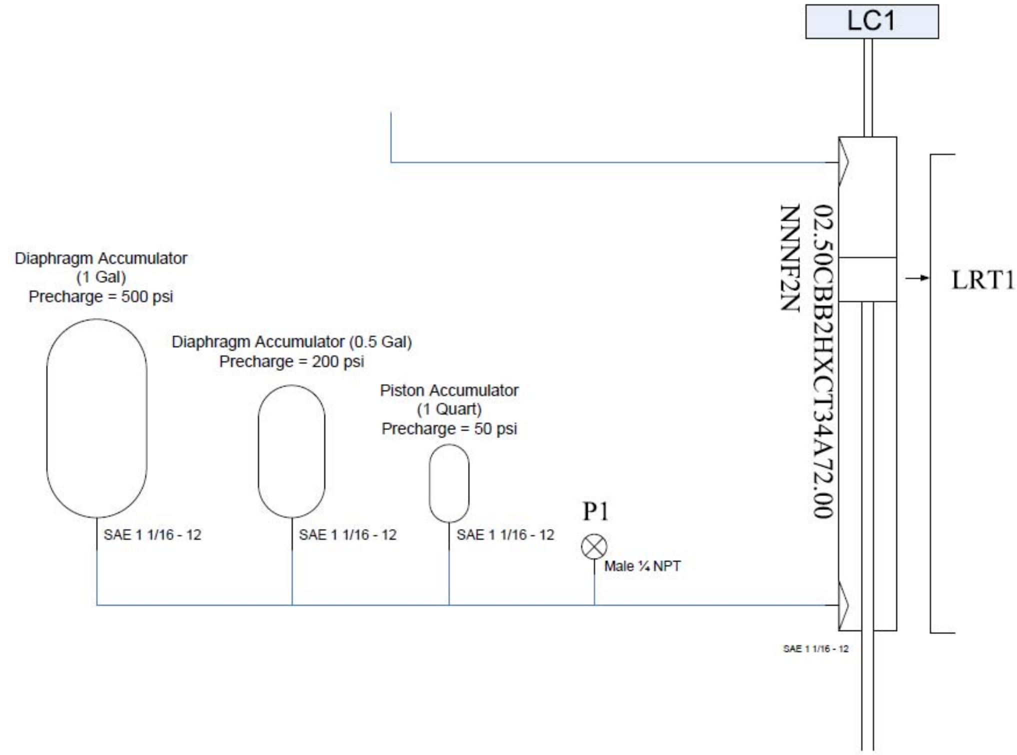


Figure 2. Schematic drawing of the hydraulic components showing the ram, the accumulator system, load cell (LC1), pressure sensor (P1) and potentiometer (LRT1).

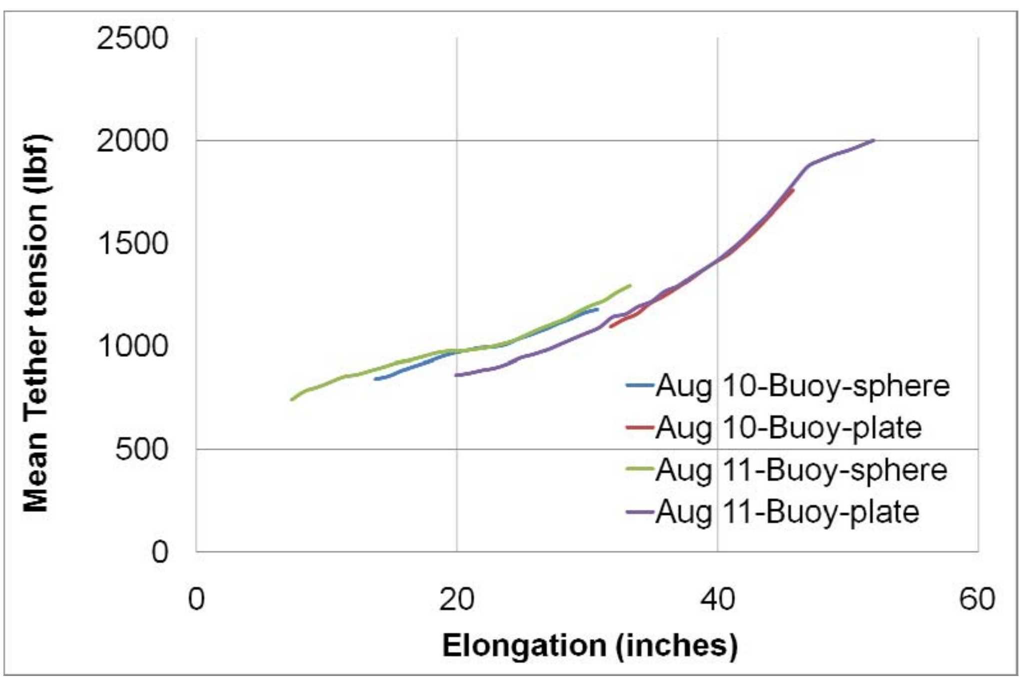


Figure 3. Experimental measurements of mean tether tension as a function of tether elongation.

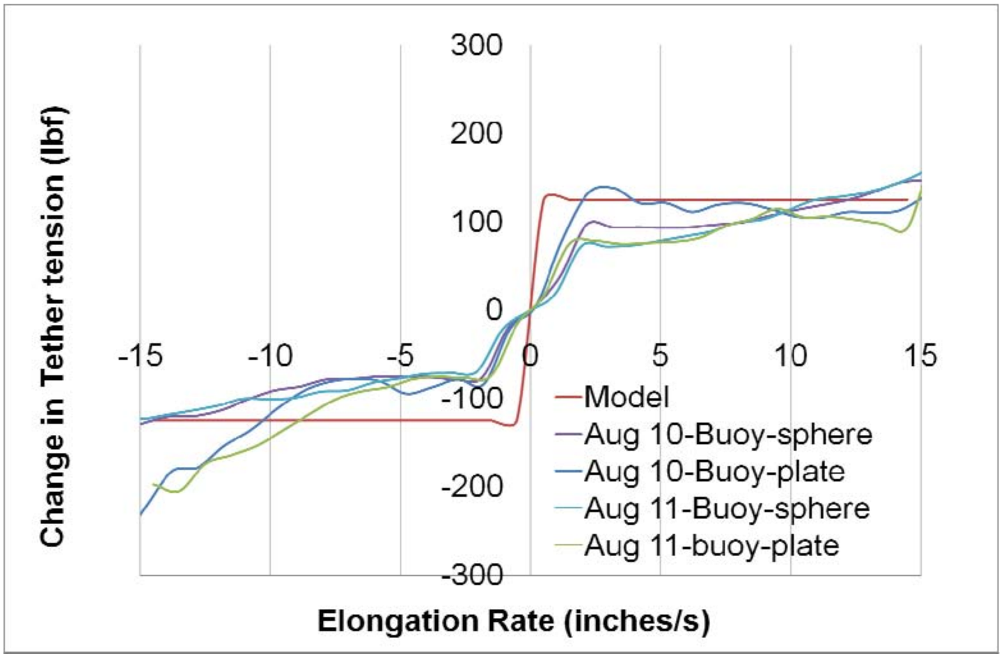


Figure 4. Variation of tether tension about the mean value in Figure 3 measured at variable tether elongation rates.

To measure the actual tensions in the system, a load cell was bolted to the lower end of the bridle to measure the tension force acting on the tether connecting the submerged element to the surface float (see figure 1). The stroke of the hydraulic ram and the resulting tether elongation was measured by a built-in potentiometer in the hydraulic ram.

The incoming wave field was measured by a nearby wave-measurement buoy. A significant wave height of 1.0 m at a peak period of 7.2 seconds were recorded on August 10th near the experimental site whereas the wave conditions were considerably milder on August 11th with the significant wave height and peak period values being 0.7 m and 8 seconds respectively. The wave spectral plots appear in figures 7 to 10. Field experimental results are sub-divided into four datasets for the ease of understanding, namely, Buoy-plate August 10th, Buoy-plate August 11th, Buoy-sphere August 10th and Buoy-sphere August 11th.

All quantities of tension, pressure and elongation were logged on-board the buoy at 100Hz for later analysis.

**Additional Calibration Information**
Figure 5 shows the calibration chart of the potentiometer built into the hydraulic ram used to measure the elongation of the tether connecting the surface buoy to the submerged element. Voltage changes nearly linearly with elongation. An extension of approximately 15 inches changes the measured voltage by 1 volt.

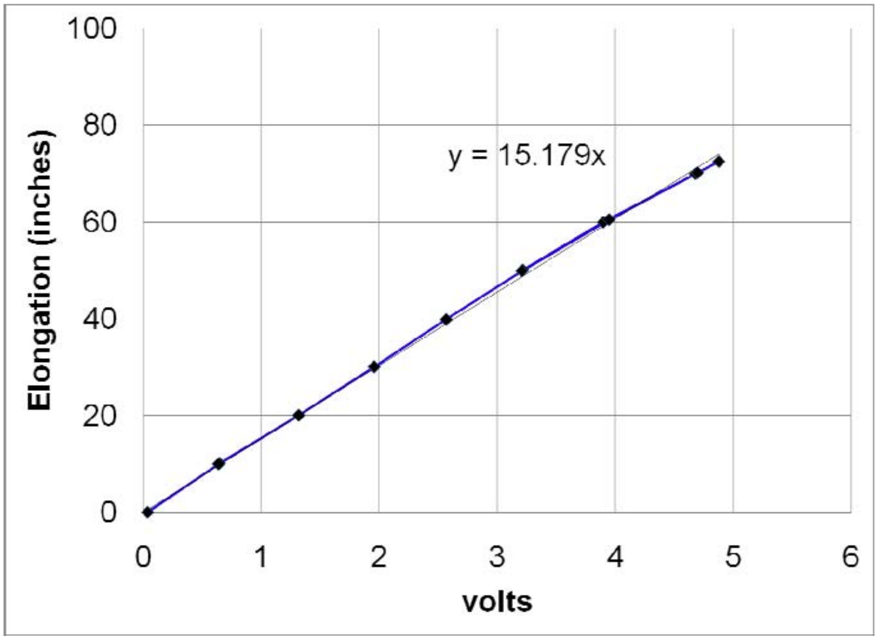


Figure 5. Experimental measurement of potentiometer calibration

## Numerical Model

The numerical model consists of an equation of motion solver that computes the resulting motion in three dimensions of a collection of floating and submerged bodies that are subject to external forcing acting on the various bodies that make up the system. The forces acting on the surface buoy include weight, hydrostatic force, wave-exciting force, wave radiation force, skin-friction and pressure drag and the tether tension. The submerged element (sphere/plate) is forced by weight, hydrostatic force, skin-friction and pressure drag and the tether tension. The hydrodynamic frequency-domain coefficients were calculated by using WAMIT Version 6.4. WAMIT is a radiation/diffraction code developed for the analysis of the interaction of surface waves with floating bodies. A separate utility was used to evaluate time-domain impulse response functions from the outputs of WAMIT.

## Results and Discussion

Two types of tests were performed for the purpose of validating the numerical model. A step response test was conducted in the MBARI test tank and two days of testing was performed at sea to measure the systems response to ocean waves.

### Step Response test

The step response experiment was conducted in the MBARI test tank on the Buoy-plate system, the buoy was lifted to a height of 12 inches and released. Experimental and modeling results of the step response test are presented in figure 6. There is excellent agreement in the phase of the motion response and tether elongation but the magnitude of tether tension is underestimated in the modeled results. This discrepancy is most likely due to the fact that the elongation rates are very high step response tests and the modeled results fails to accurately simulate the damping forces in the ram at a very high rate of tether elongation. The tension results show a high frequency disturbance at the two and four second marks. Based on observation of video of the tests, this interaction appears to be the effect of waves reflecting from the walls of the test tank.

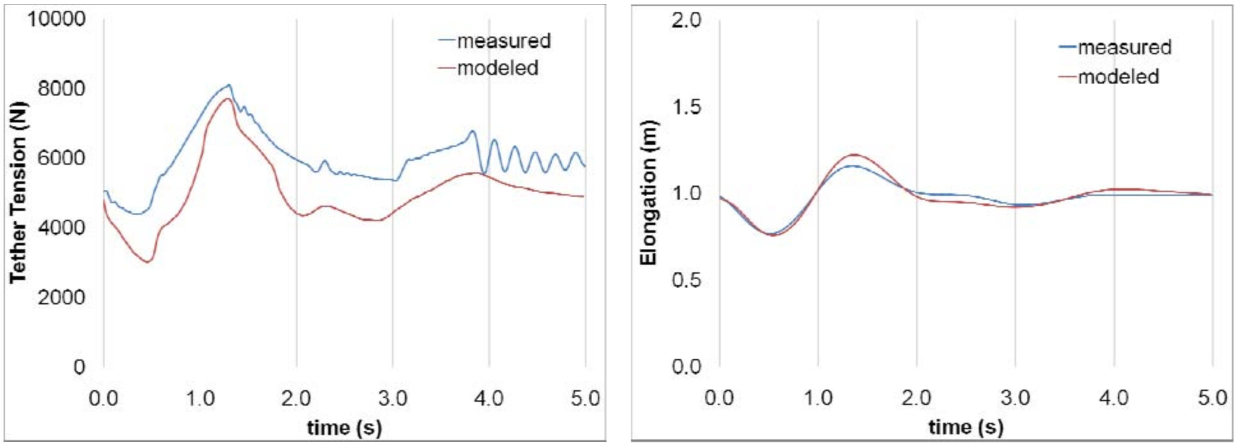


Figure 6. Experimental measurements and model generated values of tether tension and elongation during the step response test.

**Monterey Bay Field experiment**

Experimental measurements and modeling results of the systems tension and elongation response are plotted in figures 7 to 10 along with concurrent measurements of wave time history and spectra. Comparisons were made for the purposes of validating the numerical modeling results against the experimental observations of tether tension. To accurately model the hydraulic ram dynamics, the experimental observations of spring and damping force as a function of elongation and elongation rate respectively were incorporated into the model. Laboratory experiments were also conducted for confirming the spring and damping forces observed in the field experiments. At small elongation rates, the hydraulic ram dynamics was well understood. At rates exceeding 10 inches/s, there was some amount of uncertainty in the dynamic behavior of the hydraulic ram.

Comparison of experimental observations with numerical modeling results indicates reasonably good agreement. The simplified numerical model captures the buoy-plate and the buoy-sphere system hydrodynamics fairly well as illustrated in figures 7 to 10. In all cases the elongation and tension spectra have a pronounced peak at a frequency that is higher than the peak of the incoming wave spectra, this appears to be related to the natural frequency of the tether system.

The motion of the submerged body attached to the hydraulic ram can be analyzed as a single degree of freedom system oscillating along the heave direction. In this case the natural frequency of the hydraulic cylinder motion is given by

$$f_n = \frac{1}{2\pi}\sqrt{\frac{k}{m+a}} \tag{1}$$

where $f_n$ = natural frequency in Hertz
$k$ = Spring stiffness (N/m)
$m$ = mass of the submerged object (kg)
$a$ = added mass of the submerged object (kg)

Table 1 shows the expected natural frequency of the two configurations based upon linearized estimates of spring stiffness based upon the measured values of force versus elongation shown in figure 3.

| *Submerged Body* | *k (N/m)* | *m (kg)* | *a (kg)* | *Tn (s)* | *fn (Hz)* |
|---|---|---|---|---|---|
| Circular Plate | 4879.6 | 588.3 | 632.2 | 3.14 | 0.32 |
| Sphere | 2065.0 | 533.0 | 193.1 | 3.73 | 0.27 |

Table 1. Linearized hydraulic ram oscillation characteristics.

Results show that a near-zero frequency response exists when the wave exciting force is not high enough to overcome the frictional force which causes the ram to get stuck at one particular location for several seconds. For a buoy-sphere system, the variation of tether tension due to the oscillatory wave motion is about half of that of the buoy-plate system. Lower tension variation causes several instances of mechanical stiction to occur. On the other hand, tether elongation measurements for the buoy-plate system show very little stiction. The numerical model is not able to replicate the stiction mechanism observed in experiments and therefore, the near-zero frequency response is absent in the modeling results. Instead, it is represented as a low amplitude time variation in the plot of elongation with time.

The hydrodynamic damping force acting on the sphere is much lower in magnitude as compared to that of a flat plate. As a result, it takes considerably longer for the sphere to come to rest at the equilibrium position. The rate of tether elongation remains linear for small variations in tether tension and tends to become constant at higher values. Due to low damping, it does not become non-linear. For the system with a flat plate as the submerged element, high damping values tend to introduce non-linearity for large variations in tether tension. The non-linear frequency response is observed in experimental measurements at frequencies higher than the wave excitation frequencies.

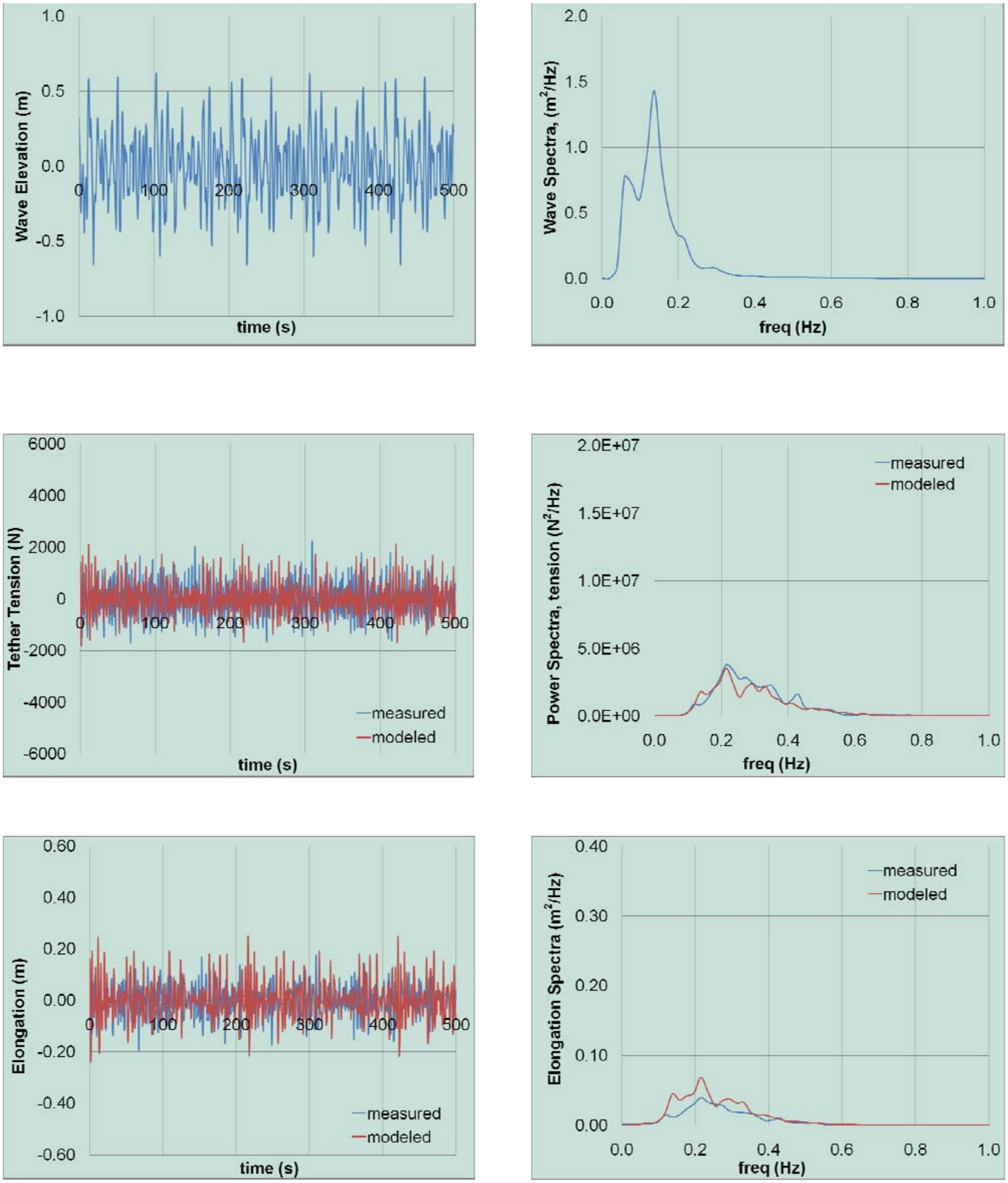


Figure 7. Time history and corresponding spectra of wave elevation, measured and modeled tether tension and elongation. (Buoy-plate Aug 11, 2009)

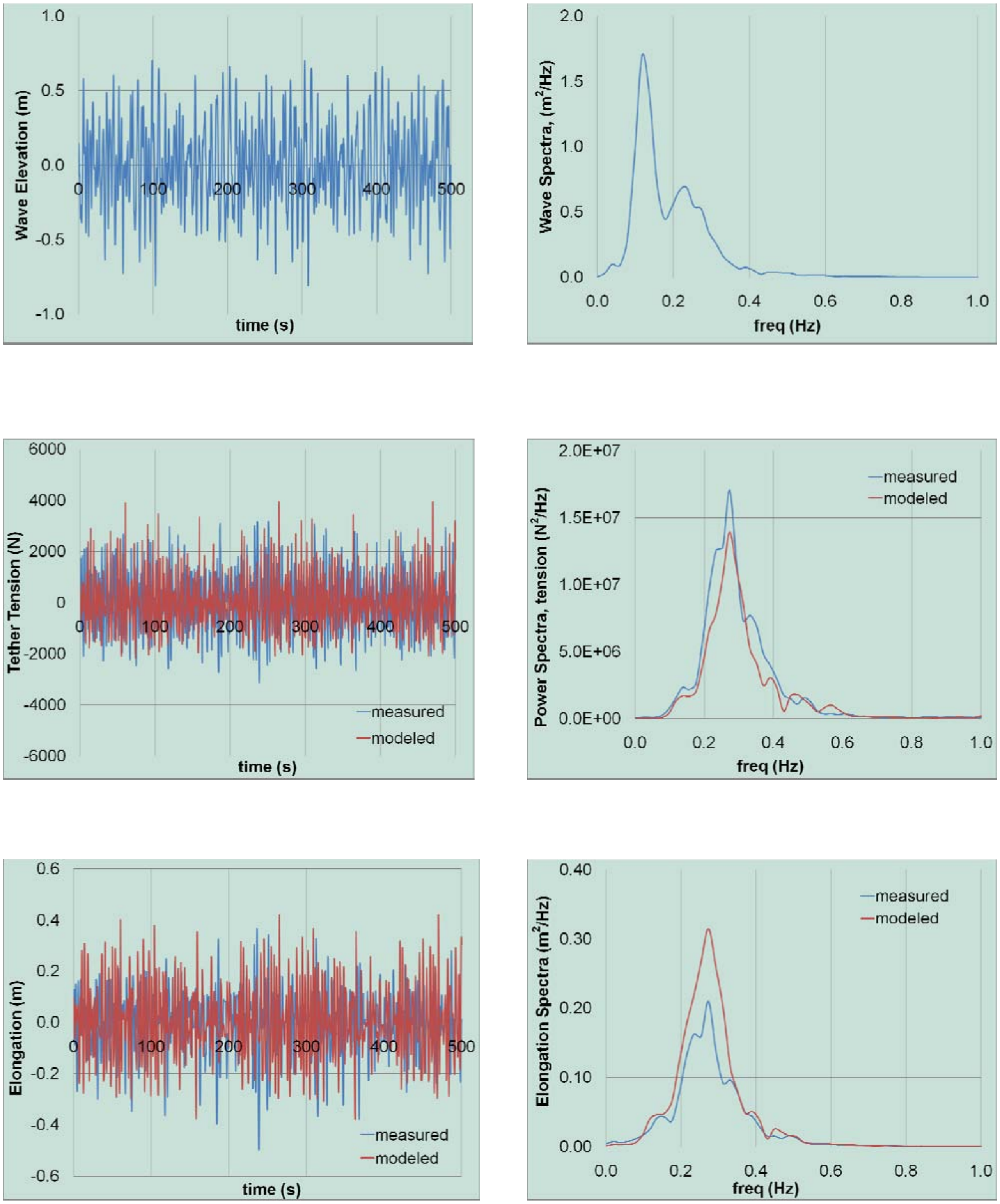


Figure 8. Time history and corresponding spectra of wave elevation, measured and modeled tether tension and elongation. (Buoy-plate Aug 10, 2009)

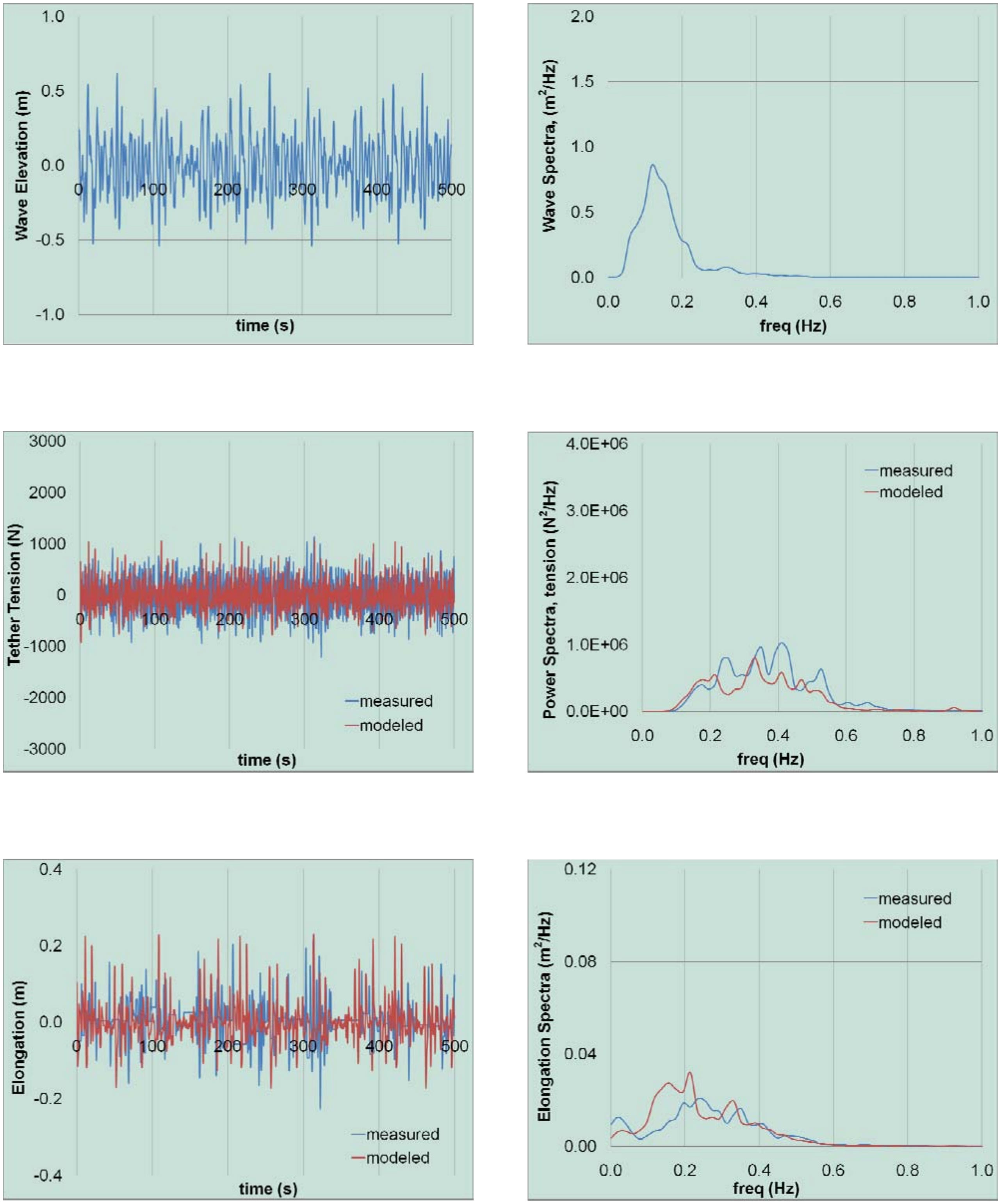


Figure 9. Time history and corresponding spectra of wave elevation, measured and modeled tether tension and elongation. (Buoy-sphere Aug 11, 2009)

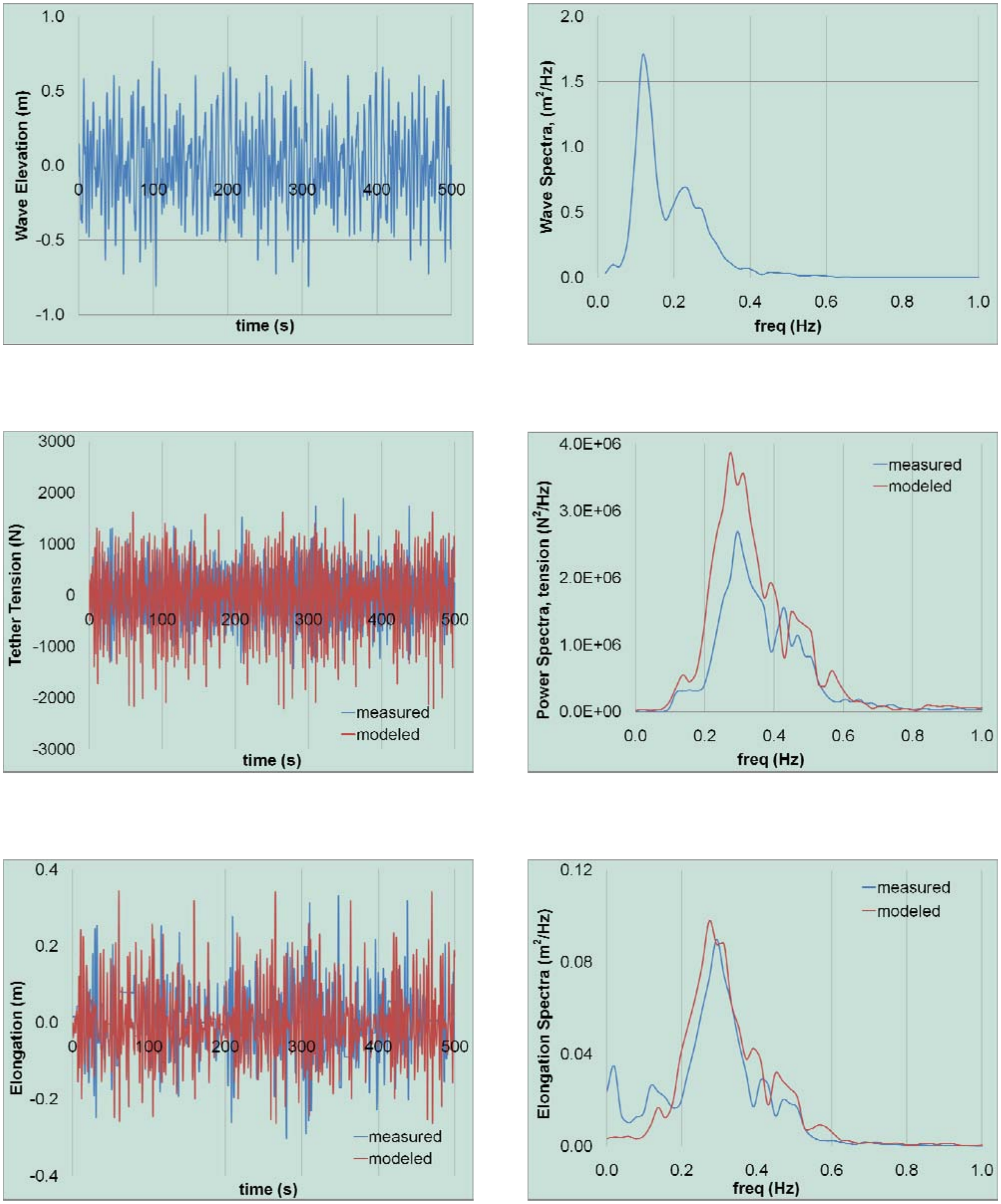


Figure 10. Time history and corresponding spectra of wave elevation, measured and modeled tether tension and elongation. (Buoy-sphere Aug 10, 2009